ac-Driven Atomic Quantum Motor

A. V. Ponomarev, S. Denisov, and P. Hänggi

Institute of Physics, University of Augsburg, Universitätstrasse 1, D-86159 Augsburg, Germany

(Received 3 February 2009; revised manuscript received 10 April 2009; published 8 June 2009)

We propose an ac-driven quantum motor consisting of two different, interacting ultracold atoms placed into a ring-shaped optical lattice and submerged in a pulsating magnetic field. While the first atom carries a current, the second one serves as a quantum starter. For fixed zero-momentum initial conditions the asymptotic carrier velocity converges to a unique nonzero value. We also demonstrate that this quantum motor performs work against a constant load.

DOI: 10.1103/PhysRevLett.102.230601 PACS numbers: 05.60.−k, 37.10.Jk, 84.50.+d

Linear or rotational motion presents the basic working principle powering all sorts of machines. For nearly two centuries, since the invention of the first electrical motor [1], the ever continuing miniaturization of devices has had profound consequences for several branches of science, industry, and everyday life. This process has already passed the scale of micrometers [2] and has entered the realm of the world of nanoscale [3]. Bioinspired devices such as chemical or light driven synthetic molecular motors identify just one of those recent successes [4]. While the operational description of such molecular motors mainly rests on classical concepts, much less is known for operational schemes that are *fully* quantum mechanical in nature. An ideal resource for the latter possibility is the dynamics of cold atoms that are positioned in optical potentials [5].

With this work, we put forward a setup for a quantum motor which consists of two species of interacting, distinguishable quantum particles that are loaded into a ring-shaped optical potential. The blueprint for such an underlying ring-shaped one-dimensional optical lattice has been proposed recently [6] and a first experimental realization has been reported in [7]. Here, we employ this setup to devise an engine which works as a genuine ac-driven quantum motor.

ac-quantum motor.—Figure 1 outlines our device. The ring-shaped optical potential, which results either from the interference of a Laguerre-Gauss (LG) laser beam with a plane wave [6] or, alternatively, of two collinear LG beams with different frequencies [7], is capable of trapping two interacting atoms. One of the atoms, termed ''carrier,'' c, is driven by an external field, while the other atom, termed ''starter,'' s, interacts locally via elastic s-wave collisions with the carrier but remains unaffected by the driving field [8]. Two possible setups that come to mind are (i) a neutral starter and an ionized carrier, a suitable driving field can be implemented in a way typically done for electrons placed in a conducting ring, i.e., by a time-dependent magnetic flux threading the lattice [9], and (ii) a spinless starter and a carrier atom with a nonzero spin which is driven by a time-dependent cone-shaped magnetic field of an Ioffe-Pritchard trap [6,10].

We next assume that both atoms are loaded into the lowest energy band of a deep, ring-shaped optical potential with L lattice sites and the lattice constant d. The time-dependent homogeneous vector potential $\tilde{A}(t)$ does not induce any appreciable transitions between the ground band and the excited band(s).

The ac-driven, total Hamiltonian H_{tot} of the motor,

$$H_{\mathrm{tot}} = H_c(t) + H_s + H_{\mathrm{int}}, \tag{1}$$

is composed of the time-dependent Hamiltonian $H_c(t)$ for the carrier

$$H_c(t) = -\frac{J_c}{2}\left(\sum_{l_c=1}^{L} e^{i\tilde{A}(t)}|l_c+1\rangle\langle l_c| + \mathrm{H.c.}\right)\otimes \mathbf{1}_s, \tag{2}$$

and for the starter H_s, respectively, i.e.,

$$H_s = -\frac{J_s}{2}\left(\sum_{l_s=1}^{L} |l_s+1\rangle\langle l_s| + \mathrm{H.c.}\right)\otimes \mathbf{1}_c. \tag{3}$$

Here, J_c and J_s are the corresponding hopping strengths which are functions of the atom masses and the optical potential depth [11]. The salient carrier-starter (on-site) interaction reads

$$H_{\mathrm{int}} = W\sum_{l_c,l_s=1}^{L} \delta_{l_c,l_s}|l_c\rangle\langle l_c|\otimes|l_s\rangle\langle l_s|, \tag{4}$$

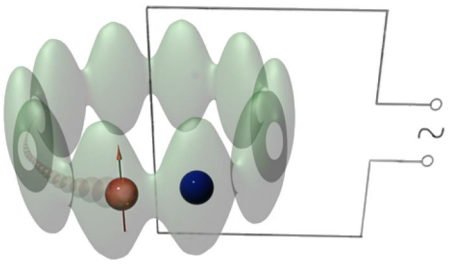

FIG. 1 (color online). Atomic quantum motor: Two different ultracold atoms are loaded into a ring-shaped optical lattice. Both atoms interact locally with each other, while only one carrier (the one with an arrow) is magnetically powered.

where W denotes the interaction strength. Throughout the remaining we use periodic boundary conditions; i.e., $|L+1\rangle = |1\rangle$. The full system Hilbert space is spanned by the direct products of single particle Wannier states $|l_c\rangle \otimes |l_s\rangle$, with the dimension being $\mathcal{N} = L^2$. The scale of the motor current will be measured in units of the maximal group velocity $v_0 = J_c d/\hbar$.

The driving of the ac-atomic quantum motor is switched on at the time instant t_0, so that the vector potential assumes the form

$$\tilde{A}(t) = \chi(t - t_0)A(t), \tag{5}$$

where $\chi(t - t_0)$ is the step function and $A(t)$ is defined on the entire time axis, $t \in (-\infty, +\infty)$.

dc-quantum current.—The mean carrier current is given as the speed of the motor by using the velocity operator: $\hat{v}_c(t) = i/\hbar[H_{\rm tot}(t), \hat{x}_c]$. With $\hat{x}_c = \sum_l l_c |l_c\rangle\langle l_c|$, one finds $\hat{v}_c(t) = -i(v_0/2)(\sum_{l_c=1}^{L} e^{iA(t)}|l_c+1\rangle\langle l_c| - \text{H.c.}) \otimes \mathbf{1}_s$. In the quasimomentum representation with $|\kappa\rangle = \sum_{n=1}^{L} \exp(i\kappa n)|n\rangle$, its quantum expectation $v_c(t;t_0) = \langle\psi(t)|\hat{v}_c(t)|\psi(t)\rangle$ reads

$$v_c(t;t_0) = v_0 \sum_{l_c=1}^{L} \rho_{\kappa_{l_c}}(t;t_0)\sin[\kappa_{l_c} + \tilde{A}(t)], \tag{6}$$

wherein $\kappa_{l_c} = 2\pi l_c/L$ is the single particle quasimomentum and where we indicated its parametric dependence on the start time t_0. Further, $\rho_{\kappa_{l_c}}(t;t_0) = \sum_{l_s} |\langle\psi(t)|\kappa_{l_s}\rangle \otimes |\kappa_{l_c}\rangle|^2$, with $\kappa_{l_s} = 2\pi l_s/L$, is the quasimomentum distribution for the carrier.

The steady state regime of the motor can be characterized by the dc component of the averaged velocity

$$v_c(t_0) := \lim_{t\to\infty} \frac{1}{t}\int_0^t v_c(t';t_0)dt'. \tag{7}$$

In the absence of the interaction between the particles, i.e., $W = 0$, and an initial preparation with localized carriers that start out with zero velocity the motor setup cannot even support a transient directed current. In fact, this result holds for *any* shape of the vector potential $A(t)$ [12]. This situation thus mimics a single-phase ac motor: a periodically pulsating magnetic field would fail to put a rotor from rest into rotation, unless one applies an initial ''push'' via a starter mechanism [13]. In our setup, the role of the quantum starter is taken over by the nonvanishing interaction W with the second particle.

Nonetheless, even with nonvanishing interaction, $|W| > 0$, there exists no evident procedure for setting the motor into rotation. A seemingly obvious solution—application of a constant carrier bias—cannot resolve the task. This is true because the corresponding vector potential, $A_B(t) = \omega_B t$, induces Bloch oscillations only [14]. In distinct contrast, we shall employ an unbiased time-dependent vector potential possessing a zero dc component, $A(t+T) = A(t)$, i.e., $\int_0^T A(\tau)d\tau = 0$.

For zero-momentum initial conditions, the unbiased monochromatic ac force, $A(t) = A\sin(\omega t)$, would launch—with equal probabilities—the system either into a clockwise (rightward) or a counterclockwise rotation (leftward motion) [15]. Thus, the *modus operandi* as a motor requires a symmetry-breaking driving field, realized here with the harmonic mixing signal,

$$A(t) = A_1\sin(\omega t) + A_2\sin(2\omega t + \Theta), \tag{8}$$

where Θ denotes the crucial symmetry-breaking phase shift. The input (8) knowingly may induce a nonvanishing nonlinear response, the so-called *ratchet effect* [15–17].

Quantum current in terms of Floquet states.—The dynamics at times $t > t_0$ of the time-periodic Hamiltonian (1) can be analyzed by using the Floquet formalism [18]. The solution of the eigenproblem, $U(t,t_0)|\phi_n(t;t_0;k)\rangle = \exp(-\frac{i}{\hbar}\epsilon_n t)|\phi_n(t;t_0;k)\rangle$, with the propagator $U(t,t_0) = \mathcal{T}\exp[-\frac{i}{\hbar}\int_{t_0}^{t} H_{\rm tot}(\tau)]d\tau$ ($\mathcal{T}$ denotes the time ordering), provides the set of Floquet states, being time periodic, i.e., with $T = 2\pi/\omega$ being the driving period, $|\phi_n(t+T;t_0;k)\rangle = |\phi_n(t;t_0;k)\rangle$. Here, $k = \sum_{l,m}\langle\phi_l|\kappa_l\rangle_s \otimes |\kappa_m\rangle_c$ is the *total* quasimomentum of the Floquet state. Because of the discrete translation invariance of the system, the total quasimomentum is conserved during the time evolution, thus serving as a quantum number. Since $H_{\rm tot}$ is a function of the time difference $t - t_0$ only, the quasienergies ϵ_n are independent of t_0, and the Floquet states for different start times t_0 are related by $|\phi_n(t;t_0;k)\rangle = |\phi_n(t-t_0;0;k)\rangle$.

Using this relation we next decompose $\psi(t_0)$ in the complete basis of Floquet states: $|\psi(t_0)\rangle = \sum_{n=1}^{\mathcal{N}} c_n|\phi_n(0;t_0;k)\rangle = \sum_{n=1}^{\mathcal{N}} c_n|\phi_n(T-t_0;0;k)\rangle$. In the absence of the driving, $A(t) \equiv 0$, the motor setup (1)–(3) possesses the continuous translational symmetry in time. Thus, the expansion coefficients of the initial wave function $\psi(t_0)$ in the system eigenbasis knowingly do not depend on time. On the contrary, eigenstates of a periodically driven system—the Floquet states—evolve in time, being locked by the external ac field. The expansion of an initial wave function over the Floquet eigenbasis depends on the start time t_0 (5), which determines the phase of the driving ac field [15]: $c_n = c_n(t_0) = \langle\phi_n(T-t_0,0;k)|\psi(t_0)\rangle$. Substitution of the above decomposition into (7) yields the result

$$v_c(t_0) = \sum_{n=1}^{\mathcal{N}} \bar{v}_n|c_n(t_0)|^2, \qquad \bar{v}_n = \frac{1}{T}\int_0^T v_n(\tau)d\tau. \tag{9}$$

Here, $\bar{v}_n$ denotes the quantum average velocity of the nth Floquet state (6). Because the Floquet states are periodic functions of the time difference $\tau = t - t_0$ only, the velocities $\bar{v}_n$ do not depend on t_0, and the dependence of the generated dc current on the t_0 solely stems from the coefficients $c_n(t_0)$. Since the system evolution is fully quantum coherent, i.e., there is no memory erasing induced by an environment, the asymptotic current maintains the

memory of the initial condition as encoded in the coefficients $c_n(t_0)$ [15].

Input-output characteristics.—The question is now, how can we control the motor? To answer this question, we used the symmetry analysis [15] which allows us to predict an appearance of a certain dc current. Combining time-reversal operation and the complex conjugation applied to (6) with $A(t)$ in the form of (8), one can prove the (anti) symmetric dependence of $\bar{v}_n$ on Θ for the Floquet states with $k = 0$: $\bar{v}_n(\pi - \Theta) = \bar{v}_n(\Theta)$, $\bar{v}_n(-\Theta) = -\bar{v}_n(\Theta)$. Thus, the Floquet states with $k = 0$ possess zero mean velocities at $\Theta = 0, \pi$. Furthermore, using a similar reasoning, one finds that the set of Floquet states with nonzero k can be ordered by the parity relation, which links eigenstates with opposite quasimomenta, $\phi_n(t; t_0; -k; \Theta) = \phi_m(T - t; t_0; k; -\Theta)$, yielding $\bar{v}_n = -\bar{v}_m$. This implies that, for a symmetric (in k) initial state and $\Theta = 0, \pi$, the contributions to the dc current of Floquet states with opposite quasimomenta eliminate each other. The same holds true for a monochromatic driving (8), with $A_2 = 0$ [15]. Shifting Θ away from $0, \pm\pi$ causes the decisive symmetry breaking and leads to the desymmetrization of the Floquet states with $k = 0$ and consequently will violate the parity between states with opposite signs of k.

The motor speed depends on the initial conditions, which define the contributions of different Floquet states to the carrier velocity (9). We restrict our analysis to the initial state $\psi(t_0) = L^{-1/2}|l_c\rangle \otimes \sum_{l_s}|l_s\rangle$, $l_c = 1, \ldots, L$, in the form of the localized carrier (at l_c) and the uniformly ''smeared,'' delocalized starter. Both particles have zero velocities at $t = t_0$. The asymptotic velocity typically exhibits a strong dependence on t_0 [15]. We first discuss the results obtained after averaging over t_0, thus assigning a unique motor velocity value,

$$v_c = \langle v_c(t_0)\rangle_{t_0} = 1/T \int_{t_0}^{T+t_0} v_c(t_0)dt_0, \qquad (10)$$

for fixed system parameters.

Figure 2 depicts the dependence of the average motor velocity on Θ. The results obtained by direct time propagation of the initial state and averaged over t_0 (dashed line) are superimposed by those calculated via the Floquet formalism (9) (solid line). The agreement between the two curves is satisfactory but not perfect: This is true because of the sharp peaks on the asymptotic current (9).

These peaks can be associated with *avoided crossings* between two quasienergy levels [15]. These avoided crossings cause a strong current enhancement if one of the interacting and transporting eigenstate overlaps significantly with an initial, nontransporting state of the motor. Note also that a very narrow avoided crossing requires a very large evolution time to become resolved, i.e., $t_{\rm obs} \sim \hbar/|\epsilon_\alpha - \epsilon_\beta|$ [15]. Our chosen evolution time $t = 200T$ is not large enough to clearly resolve the distinct resonances depicted in Fig. 2.

We further detect that the dependence of the motor velocity $v_c(t_0)$ in (7) on t_0 increasingly disappears upon

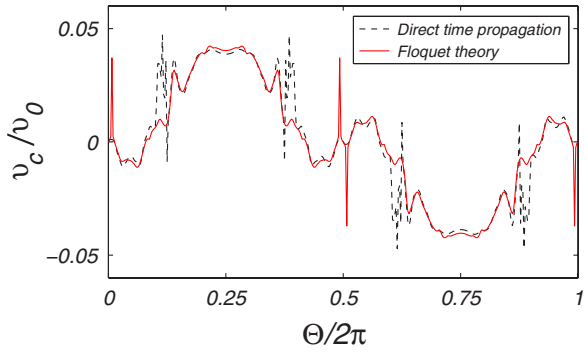

FIG. 2 (color online). Averaged motor velocity in (10) (in units of the maximal group velocity $v_0 = J_c d/\hbar$) as a function of the phase shift Θ in (8) for $L = 16$. The (t_0)-averaged velocity (7) obtained by the direct time propagation of the initial state up to $200T$ (dashed line) is compared to the asymptotic dependence given by the Floquet approach (9) (red solid line). The parameters are $\hbar\omega = 0.1J_c$, $A_1 = 0.5$, $A_2 = 0.25$, $W = 0.2J_c$, $J_s = J_c = J$.

increasing the size L (not shown). To provide a quantitative estimate, we evaluated the dispersion of the current (9) with respect to t_0, i.e.,

$$\Sigma_v = \sqrt{\langle v_c(t_0)^2 - \langle v_c(t_0)\rangle_{t_0}^2\rangle_{t_0}}. \qquad (11)$$

As shown in Fig. 3 this dispersion decays with increasing size L, being rather faint for $L \gtrsim 16$. For sizes $L \gtrsim 16$ the carrier assumes an asymptotic velocity that essentially is independent of the initial start time t_0. This effect is caused by the presence of the starter: The carrier velocity is obtained as the trace over the part of the total system Hilbert space, associated with the starter. The starter dynamics mimics a dissipative, finite heat bath for the carrier dynamics whose effectiveness increases with both the (i) the dimension of the starter subspace, i.e., the size L, and (ii) the strength of the interaction W.

Load characteristics.—The analysis based on Eqs. (1)–(3) and (8) has been for a free rotator. In order to qualify for a genuine motor device, the engine must be able to operate under an applied load. The load is introduced as the bias $\omega_B t$, being added to the vector potential $\tilde{A}(t)$. All the information about transport properties can be extracted by using again the Floquet formalism, provided that the

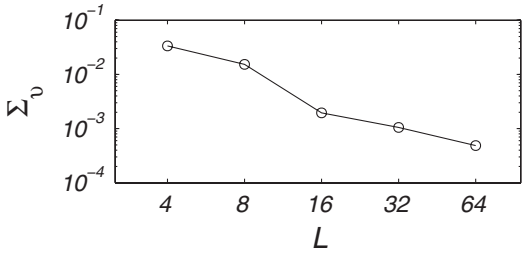

FIG. 3. Dispersion of the motor velocity (11) versus the number of lattice sites L. Here $\Theta = \pi/2$, and the other parameters are the same as in Fig. 2.

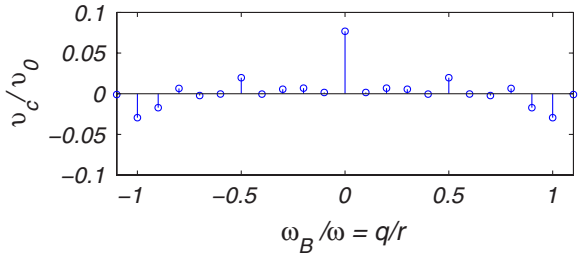

FIG. 4 (color online). The average motor velocity for "resonance" driving and an initial condition "localized carrier and delocalized starter" ($r = 10$). The parameters are $W = 0.2J_c$, $J_s = J_c = J$, $\hbar\omega = 0.1J_c$, $A_1 = 0.5$, $A_2 = 0.25$, $\Theta = \pi/2$, and $L = 4$.

ac-driving and the Bloch frequencies are mutually in resonance [19], i.e., $q\omega = r\omega_B$, where r and q are coprime integers. Figure 4 shows the dependence of the asymptotic motor speed for different bias values. There are two remarkable features. First, the spectrum of velocities is symmetric around $\omega_B = 0$. This follows because of the specific choice of the phase shift at $\Theta = \pi/2$. Second, while some regimes provide a transport velocity along the bias, others correspond to the uphill motion, against the bias. Therefore, a stationary transport in either direction is feasible. The load characteristic exhibits a discontinuous, fractal structure and, in distinct contrast to the classical case [20], it cannot be approximated by a smooth curve. This is a direct consequence of the above mentioned resonance condition.

Experimental realizations.—For an experimental realization of this quantum atom motor the following features should be respected: (i) In the case of the setup "carrier with a spin or spinless starter," the carrier should assume a magnetic number $m_F \geq 2$ [6], to efficiently induce the ac-field amplitudes $A_{1,2}$. (ii) Because in the tight-binding approximation the maximal amplitude of the tunneling is limited from above, $J_c \lesssim J_{\max} = 0.13E_0$, for ^{6}Li atom, the lattice spacing $d \sim 10$ μm [7], and $\hbar\omega = 0.1J_c$ (used in the calculations), the driving frequency ω should be less than 2 Hz. Then, the time required to launch the motor (i.e., to approach the asymptotic velocity value) is around a minute. Further focusing of the laser beam can decrease the lattice constant d, thereby decreasing the launch time to experimentally accessible coherence times around 10 sec [21].

Conclusions.—We studied a quantum ac motor made of the two species of ultracold interacting atoms, i.e., a carrier and a starter, moving in a ring-shaped trapping potential. For zero-momentum initial conditions the asymptotic carrier velocity loses its dependence on the switch-on time t_0 of the ac drive upon increasing the lattice size L. A natural question that arises is, What about the averaged starter velocity v_s? We find that the latter sensitively depends on the system parameters: It can either be very small compared to the carrier velocity or also larger than v_c. In short, the starter can move codirectionally or contradirectionally to the carrier motion. Finally, an extension of our motor setup to several interacting bosons (i.e., a finite bosonic "heat bath") presents an intriguing perspective.

We acknowledge I. V. Ponomarev for providing us with the illustration shown in Fig. 1. This work was supported by the DFG through Grant No. HA1517/31-1 and by the German Excellence Initiative "Nanosystems Initiative Munich (NIM)."

[1] The conversion of electrical energy into mechanical work by electromagnetic means was devised by Michael Faraday in 1821. The first operating electric motor was demonstrated by Ányos Jedlik in 1828.
[2] J. G. Korvink and O. Paul, *Microelectromechanical Systems* (Springer, Norwich, New York, 2006).
[3] A. M. Fennimore, Nature (London) **424**, 408 (2003); D. L. Fan, F. Q. Zhu, R. C. Cammarata, and C. L. Chien, Phys. Rev. Lett. **94**, 247208 (2005).
[4] R. A. van Delden *et al.*, Nature (London) **437**, 1337 (2005); E. R. Kay, D. A. Leigh, and F. Zerbetto, Angew. Chem., Int. Ed. **46**, 72 (2007); G. S. Kottas, L. I. Clarke, D. Horinek, and J. Michl, Chem. Rev. **105**, 1281 (2005).
[5] O. Morsch and M. Oberthaler, Rev. Mod. Phys. **78**, 179 (2006).
[6] L. Amico, A. Osterloh, and F. Cataliotti, Phys. Rev. Lett. **95**, 063201 (2005).
[7] S. Franke-Arnold *et al.*, Opt. Express **15**, 8619 (2007).
[8] For example, it can be bosonic ^{174}Yb atom, prepared in spinless ground state plus fermionic ^{171}Yb atom, see K. Honda *et al.*, Phys. Rev. A **66**, 021401(R) (2002), or bosonic ^{87}Rb plus fermionic ^{6}Li, see C. Silber *et al.*, Phys. Rev. Lett. **95**, 170408 (2005).
[9] S. Viefers *et al.*, Physica (Amsterdam) **21E**, 1 (2004).
[10] A. E. Leanhardt *et al.*, Phys. Rev. Lett. **89**, 190403 (2002).
[11] Here, for simplicity, we have assumed the limit of a deep periodic potential, also refereed to as the tight-binding model. This limit is well justified for a potential amplitude of $V_0 \gtrsim 5E_0$ ($E_0 = \hbar^2\pi^2/2Md^2$ is the "recoil" energy, M is the mass of the atom), where the higher-order tunneling amplitude is less than 10% of the leading first order (i.e., the next neighbor) tunneling amplitude [5].
[12] I. Goychuk and P. Hänggi, J. Phys. Chem. B **105**, 6642 (2001).
[13] A. Hughes, *Electric Motors and Drives* (Newnes, London, 2006), 3rd ed.
[14] A. V. Ponomarev *et al.*, Phys. Rev. Lett. **96**, 050404 (2006).
[15] S. Denisov *et al.*, Phys. Rev. A **75**, 063424 (2007).
[16] P. Hänggi and F. Marchesoni, Rev. Mod. Phys. **81**, 387 (2009).
[17] P. H. Jones, M. Goonasekera, and F. Renzoni, Phys. Rev. Lett. **93**, 073904 (2004); R. Gommers, S. Bergamini, and F. Renzoni, *ibid.* **95**, 073003 (2005); P. Sjolund *et al.*, *ibid.* **96**, 190602 (2006).
[18] M. Grifoni and P. Hänggi, Phys. Rep. **304**, 229 (1998).
[19] M. Glück, A. R. Kolovsky, and H. J. Korsch, Phys. Rep. **366**, 103 (2002).
[20] M. Kostur *et al.*, Physica (Amsterdam) **371A**, 20 (2006).
[21] M. Gustavsson *et al.*, Phys. Rev. Lett. **100**, 080404 (2008).